

# Autoantibody-induced internalization of nicotinic acetylcholine receptor $\alpha 3$ subunit exogenously expressed in human embryonic kidney cells

メタデータ	言語: eng 出版者: 公開日: 2017-10-05 キーワード (Ja): キーワード (En): 作成者: メールアドレス: 所属:
URL	<a href="http://hdl.handle.net/2297/33430">http://hdl.handle.net/2297/33430</a>

## **Autoantibody-mediated internalization of nicotinic acetylcholine receptor $\alpha 3$**

### **subunit exogenously expressed in human embryonic kidney cells**

Shota Kobayashi<sup>a, b</sup>, Shigeru Yokoyama<sup>c</sup>, Takahiro Maruta<sup>d</sup>, Masako Negami<sup>e</sup>, Akiko

Muroyama<sup>a</sup>, Yasuhide Mitsumoto<sup>a</sup>, Kazuo Iwasa<sup>f</sup>, Masahito Yamada<sup>f</sup>, Hiroaki

Yoshikawa<sup>b, f\*</sup>

<sup>a</sup> *Laboratory of Alternative Medicine and Experimental Therapeutics, Department of Clinical Pharmacy, Faculty of Pharmaceutical Sciences, Hokuriku University, Kanazawa, Ishikawa 920-1181, Japan*

<sup>b</sup> *Health Service Center, Kanazawa University, Kanazawa, Ishikawa 920-1192, Japan*

<sup>c</sup> *Department of Biophysical Genetics, Kanazawa University Graduate School of Medicine, Kanazawa, Ishikawa 920-8640, Japan*

<sup>d</sup> *Neurological Center, Kanazawa Nishi Hospital, Kanazawa, Ishikawa 920-0025, Japan*

<sup>e</sup> *Keiju Medical Center, Nanao, Ishikawa 926-8605, Japan*

<sup>f</sup> *Department of Neurology and Neurobiology of Aging, Kanazawa University Graduate School of Medical Science, Kanazawa, Ishikawa 920-0025, Japan*

\*Corresponding author: Health Service Center, Kanazawa University, Kanazawa, Ishikawa 920-1192, Japan. Tel.: +81-76-264-5254; fax: +81-76-234-4044

E-mail address: hiroaki@staff.kanazawa-u.ac.jp

## **Abstract**

Autoantibody against nicotinic acetylcholine receptor (nAChR)  $\alpha 3$  subunit has been implicated in paraneoplastic neurological syndrome. It has been proposed that this autoantibody impairs synaptic transmission, probably by inducing the internalization of nAChR. To confirm this hypothesis, we incubated human embryonic kidney cells exogenously expressing  $\alpha 3$  subunit with seropositive serum, and visualized the intracellular localization of IgG and  $\alpha 3$  subunits by double-labeled immunofluorescence staining. As a result, co-localization of internalized IgG and  $\alpha 3$  subunits was observed as overlapping punctate fluorescent staining. Our results suggest that autoantibodies against nAChR  $\alpha 3$  subunit play a pathogenic role in synaptic transmission by inducing nAChR internalization.

*Keywords:* nicotinic acetylcholine receptor  $\alpha 3$  subunit, autoantibody, receptor internalization

## 1. Introduction

Autoantibody against nicotinic acetylcholine receptor (nAChR)  $\alpha 3$  subunit has been implicated in paraneoplastic neurological syndrome (Vernino et al., 1998; McKeon et al., 2009). This autoantibody is also known as ‘anti-ganglionic nAChR autoantibody’ because it was first detected as an autoantibody specific for neuronal nAChR expressed in autonomic ganglia (Vernino et al., 2000). Some clinical and serological studies have revealed the positive correlation between serum levels of this autoantibody and the severity of autonomic symptoms including orthostatic hypotension, gastrointestinal hypomotility and sudomotor dysfunction (Klein et al., 2003; Winston and Vernino, 2010). In addition, recent studies have reported the presence of diverse neurological symptoms unrelated to autonomic nervous systems, such as peripheral neuropathy and psychiatric symptoms, in seropositive patients (McKeon et al., 2009; Gibbons et al., 2012).

Neuronal nAChRs are ligand-gated cation channels that mediate fast synaptic transmission. They are assembled as a homomeric or heteromeric pentamer from  $\alpha$  ( $\alpha 2$ - $\alpha 10$ ) and  $\beta$  ( $\beta 2$ - $\beta 4$ ) subunits (Albuquerque et al., 2009). The  $\alpha 3$  subunits are

widely distributed in both central and peripheral nervous systems (Flores et al., 1996; Genzen et al., 2001; Skok, 2002; Khan et al., 2003), where they are expressed in various combinations with  $\alpha 5$ ,  $\beta 2$  and  $\beta 4$  subunits (Albuquerque et al., 2009). The wide distribution of  $\alpha 3$  subunits may explain the diversity of neurological symptoms observed in seropositive patients. On the other hand, autoimmunity to  $\alpha 4$  and  $\alpha 7$  subunits has been thought to be involved in some neurological disorders, such as encephalopathy and cognitive impairment (Baker et al., 2009; Lykhmus et al., 2011).

There is increasing evidence that autoantibody-mediated dysfunction of nAChR is associated with the neurological symptoms observed in seropositive patients. Some electrophysiological studies both *in vivo* and *in vitro* have revealed the pathogenic roles of anti-nAChR  $\alpha 3$  subunit autoantibody. Rabbits immunized with recombinant  $\alpha 3$  subunits (Lennon et al., 2003) and mice given anti-nAChR  $\alpha 3$  subunit autoantibodies by passive transfer (Vernino et al., 2004; Wang et al., 2010) developed autonomic dysfunction and showed the impairment of cholinergic neurotransmission. It was suggested that cross-linking and internalization of cell-surface nAChR mainly contribute to the impairment of nAChR current (Wang et al., 2007). However, there is

no evidence for autoantibody-mediated internalization of  $\alpha 3$  subunits so far.

Therefore, we examined the internalization of IgG and the  $\alpha 3$  subunit using a seropositive patient's serum by double-labeled immunofluorescence staining. To examine the specific contribution of the autoantibody to the  $\alpha 3$  subunits, we carried out experiments on human embryonic kidney (HEK) 293 cells stably co-expressing  $\alpha 3$  and  $\beta 4$  subunits. The seropositive patient's serum used in this study was confirmed to include IgG specifically recognizing the  $\alpha 3$  subunit. This study reinforces the idea that autoantibody against neuronal nAChR contributes to pathogenic processes by affecting cell-surface nAChR  $\alpha 3$  subunits.

## **2. Materials and methods**

### *2.1. Serum samples*

Serum was collected from a patient with paraneoplastic neurological disorder who was seropositive for anti-ganglionic nAChR autoantibody. The titer of the autoantibody was estimated to be 2.20 nmol/L (normal < 0.05 nmol/L) by the radioimmunoprecipitation assay described in a previous report (Vernino et al., 2008). Three samples of normal sera were obtained from healthy volunteers who received an annual health checkup at Keiju Medical Center (Nanao, Japan). Informed consent for this study was obtained from all subjects. This study was performed under the approval of the Medical Ethics Committee of Kanazawa University.

### *2.2. Construction of expression plasmids*

cDNA fragments encoding human nAChR  $\alpha 3$ ,  $\alpha 4$ ,  $\alpha 5$ ,  $\alpha 7$ ,  $\beta 2$  and  $\beta 4$  subunits were obtained by reverse transcription-polymerase chain reaction (RT-PCR) as follows. Human brain total RNA (Clontech, Mountain View, CA, USA) was reverse-transcribed using Transcriptor First Strand cDNA Synthesis Kit (Roche Applied Science,

Mannheim, Germany) according to the manufacturer's protocol. The resulting cDNA was then subjected to nested PCR using two sets of primers specific for each subunit (Table 1). Each reaction mixture (50  $\mu$ l) contained cDNA (corresponding to 10 ng of total RNA), KOD FX buffer (Toyobo, Osaka, Japan), 200  $\mu$ M dNTPs, 300 nM each primer and KOD FX DNA polymerase (Toyobo). Amplification was carried out in a thermal cycler (Applied Biosystems, Foster City, CA, USA) with the following protocol: initial denaturation at 96°C for 1 min, followed by 30 cycles of 10 sec at 98°C, 30 sec at 65°C and 2 min at 68°C. The resulting PCR products were purified using MinElute PCR Purification Kit (QIAGEN, Hilden, Germany). After addition of deoxyadenosine to the 3' ends using Ex Taq polymerase (Takara Shuzo, Otsu, Japan), the cDNA fragments encoding nAChR  $\alpha$ 3,  $\alpha$ 4,  $\alpha$ 5,  $\alpha$ 7,  $\beta$ 2 and  $\beta$ 4 subunits were cloned into a pCR2.1-TOPO vector (Invitrogen, Carlsbad, CA, USA) using a TOPO TA Cloning Kit (Invitrogen) according to the manufacturer's protocol, to yield pTOPO-CHRNA3, pTOPO-CHRNA4, pTOPO-CHRNA5, pTOPO-CHRNA7, pTOPO-CHRNB2 and pTOPO-CHRNB4, respectively. The cDNA inserts were verified by nucleotide sequencing. The 1.5-kb *Eco*RI fragments from

pTOPO-CHRNA3 and pTOPO-CHRN4 were cloned into the *EcoRI* site of pcDNA3.1 (+) (Invitrogen); the resulting plasmids were designated pcDNA-CHRNA3 and pcDNA-CHRN4, respectively. In addition, the 1.5-, 1.9-, 1.5-, 1.5- and 1.5-kb *EcoRI* fragments from pTOPO-CHRNA3, pTOPO-CHRNA4, pTOPO-CHRNA5, pTOPO-CHRN2 and pTOPO-CHRN4, respectively, and the 1.5-kb *XhoI/BamHI* fragments from pTOPO-CHRNA7 were ligated to the *XbaI*-cleaved pEF-BOS (a generous gift from Professor Nagata, Kyoto University, Japan) (Mizushima and Nagata, 1990), after treatment with Klenow fragment of DNA polymerase I; likewise, the resulting plasmids were designated pEF-CHRNA3, pEF-CHRNA4, pEF-CHRNA5, pEF-CHRNA7, pEF-CHRN2 and pEF-CHRN4, respectively.

### 2.3. Cell culture and transfection

HEK293 cells were maintained in a humidified incubator with 5% CO<sub>2</sub> at 37°C in Dulbecco's modified Eagle's medium (DMEM; Wako Pure Chemical Industries, Osaka, Japan) supplemented with 10% heat-inactivated fetal bovine serum (FBS; Gibco-BRL, Grand Island, NY, USA), 100 units/ml penicillin and 0.1 mg/ml streptomycin (Wako

Pure Chemical Industries).

For transient transfection, COS-7 cells were seeded at a density of  $1.0 \times 10^4$  cells/cm<sup>2</sup> on poly-L-ornithine (PLO; Sigma-Aldrich, St. Louis, MO, USA)-coated glass coverslips or 100-mm culture dishes. Twenty-four hours after seeding, cells were transiently transfected with pEF-CHRNA3, pEF-CHRNA4, pEF-CHRNA5, pEF-CHRNA7, pEF-CHRN2, pEF-CHRN4 and empty vector (mock) using FuGENE6 Transfection Reagent (Roche Applied Science) according to the manufacturer's protocol. Forty-eight hours after transfection, cells were subjected to autoantibody detection by immunofluorescence staining and immunoblot analysis.

For stable transfection, HEK293 cells were seeded at a density of  $1.0 \times 10^4$  cells/cm<sup>2</sup> on 100-mm culture dishes. Forty-eight hours after seeding, cells were co-transfected with pcDNA-CHRNA3 and pcDNA-CHRN4, or transfected with an empty vector (mock) using FuGENE6 Transfection Reagent. Forty-eight hours after transfection, culture medium was replaced with DMEM containing 10% FBS and 800 µg/ml G418 (Roche Applied Science). Cell colonies resistant to G418 were isolated and maintained in DMEM containing 10% FBS and 100 µg/ml G418. Co-expression

of  $\alpha 3$  and  $\beta 4$  subunits was confirmed by both immunofluorescence staining and immunoblot analysis.

#### *2.4. Immunofluorescence staining*

COS-7 and HEK293 cells were grown on PLO-coated glass coverslips, fixed in ice-cold 4% paraformaldehyde (PFA) for 20 min, washed in PBS, three changes, each 10 min, blocked in PBS containing 1% BSA and 0.3% Triton X-100 for 30 min and sequentially incubated with (1) primary antibodies against each nAChR subunit (Table 2) in the blocking solution for 3 hr at room temperature (RT); (2) washing solution (PBS containing 0.3% Triton X-100), three changes, each 10 min; (3) secondary antibodies (Table 2) in the blocking solution for 1 hr at RT; and (4) washing solution, three changes, each 10 min. For staining of cell-surface nAChR subunits, Triton X-100 was omitted from all solutions. In the case of autoantibody detection, COS-7 cells were first incubated with the patient's or normal serum (1:500–10,000) overnight at 4°C, and then with secondary antibody (Table 2) for 1 hr at RT. The coverslips were mounted on glass slides with Dapi-Fluoromount-G (SouthernBiotech,

Birmingham, AL, USA). Images were captured by a BX51 fluorescence microscope (Olympus, Tokyo, Japan) using DP controller (Olympus) and processed using DP Manager (Olympus). Fluorescence Mirror Units were U-MNIBA3 (excitation, 470–495 nm; emission, 510–550 nm), U-MWIG3 (excitation, 530–550 nm; emission, 575 nm) and U-MWU2 (excitation, 330–385 nm; emission, 420 nm).

Immunofluorescent intensities were quantitated densitometrically using ImageJ software (version 1.43; National Institute of Health, Bethesda, MD, USA). The ratio of red (Alexa Fluor 594) to green (DyLight 488) fluorescent signals was calculated after subtracting green fluorescent intensities obtained from non-transfected COS-7 cells. One hundred and eighty cells were analyzed in twenty-eight random fields obtained from two independent experiments.

### *2.5. Immunoblot analysis*

COS-7 and HEK293 cells on culture plates were harvested by scraping in PBS containing 0.1% (w/v) EDTA and pelleted by centrifugation at  $1,500 \times g$  for 5 min at 4°C. The pellets were homogenized in ice-cold homogenization solution containing

0.32 M sucrose, 2 mM EDTA, 2 mM EGTA, 20 mM HEPES and protease inhibitor cocktail (BioVision Research Products, Milpitas, CA, USA) at pH 7.2 using a Dounce homogenizer. Protein concentration of homogenates was determined using DC protein assay (BIO-RAD, Hercules, CA, USA). The homogenates were solubilized in Laemmli sample buffer, subjected to 10% SDS-polyacrylamide gel electrophoresis (SDS-PAGE) and transferred onto polyvinylidene difluoride membranes (Millipore, Billerica, MA, USA). Then, the blots were blocked in TBS containing 3% BSA and 0.04% NP-40 for 1 hr and sequentially incubated in (1) primary antibody (Table 2) or serum (1:100) in antibody-incubation solution (TBS containing 1% BSA and 0.04% NP-40) overnight at 4°C; (2) washing solution (TBS containing 0.04% NP-40), three changes, each 15 min; (3) secondary antibodies (Table 2) in antibody-incubation solution for 1 hr at RT; and (4) washing solution, three changes, each 15 min. The blots were developed using AP color development reagent (BIO-RAD).

#### *2.6. Assay for antibody-mediated internalization of nAChR $\alpha$ 3 subunit*

HEK293 cells stably co-expressing  $\alpha 3$  and  $\beta 4$  subunits (HEK293- $\alpha 3\beta 4$ ) and mock-transfected cells were seeded at a density of  $5.0 \times 10^4$  cells/cm<sup>2</sup> on PLO-coated glass coverslips in a 24-well culture plate. On the second day, the cells were washed in PBS and incubated with heat-inactivated serum (5%) or rat anti-nAChR  $\alpha 3$  monoclonal antibody (1  $\mu$ g/ml; Abcam, Cambridge, UK) in the culture medium for 30 min at 4°C or 37°C. CELL LAB Rat IgG Isotype Control (Beckman Coulter, Brea, CA, USA) was used as a negative control for the rat anti-nAChR  $\alpha 3$  monoclonal antibody. The cells were then subjected to immunofluorescence staining using secondary antibody for human and rat IgG (Table 2). For double-labeled immunofluorescence staining, the cells were stained with antibody against nAChR  $\alpha 3$  subunit and Alexa Fluor 594-conjugated secondary antibody (Table 2). To evaluate the autoantibody-mediated internalization of nAChR  $\alpha 3$  subunits, the number of overlapping punctate dots per cell was counted under a fluorescence microscope. We counted 200 cells in eight random fields obtained from two independent experiments.

### *2.7. Statistical analysis*

Data are shown as mean  $\pm$  S.D. Results were compared using two-tailed *t*-test.

The analyses were performed with the statistical analysis system StatMateIII (ATMS Co., Ltd., Tokyo, Japan).

### **3. Results**

#### *3.1. Detection of autoantibodies against neuronal nAChR subunit*

Using sera from a patient with paraneoplastic neurological syndrome or normal volunteers and commercial antibodies, we performed double-labeled immunofluorescence staining on COS-7 cells transiently expressing  $\alpha$ 3,  $\alpha$ 4,  $\alpha$ 5,  $\alpha$ 7,  $\beta$ 2 and  $\beta$ 4 subunits (Fig. 1). Overlapping staining of human IgG and  $\alpha$ 3 subunit was observed in the patient's serum, but not in normal serum (Fig. 1A). Fig. 1B shows the relationship between serial serum dilution (1:500–10,000) and relative fluorescent intensities of human IgG. Reduction of relative immunofluorescent intensities was observed in the serial dilution of the patient's serum, but not in that of normal serum. Staining of the patient's IgG was not detected in the cells expressing  $\alpha$ 4,  $\alpha$ 5,  $\alpha$ 7,  $\beta$ 2 and  $\beta$ 4 subunits (Fig. 1C). These results clearly suggested the presence of autoantibodies

against  $\alpha 3$  subunit in the patient's serum, but not in the normal sera.

We also performed immunoblot analysis to examine the affinity of the patient's IgG for the  $\alpha 3$  subunit (Fig. 2). We confirmed the expression of  $\alpha 3$  subunit in COS-7 cells using commercial antibody. Two main protein bands with predicted molecular masses of 50 kD and 55 kD were detected in the COS-7 cells transfected with pEF-CHRNA3, but not in the mock-transfected cells (Fig. 2A). In the patient's serum, a similar blot pattern of recognition was found with anti-human IgG3 antibody, but not with anti-human IgG1, 2 and 4 antibodies (Fig. 2B).

### *3.2. Stable co-expression of nAChR $\alpha 3$ and $\beta 4$ subunits in HEK293 cells*

To examine the autoantibody-mediated internalization of  $\alpha 3$  subunit, we established HEK293 cells stably co-expressing  $\alpha 3$  and  $\beta 4$  subunits (HEK293- $\alpha 3\beta 4$ ). We confirmed the co-expression of both subunits by immunoblot analysis and immunofluorescence staining (Fig. 3). Fig. 3A shows the result of immunoblot analysis. The predicted bands of  $\alpha 3$  (50 kD) and  $\beta 4$  (55 kD) were detected in HEK293- $\alpha 3\beta 4$  cells, but not in mock-transfected cells. The band at 42 kD is most

likely a proteolytic form of  $\beta 4$  subunit. The bands at 38 kD and 70 kD might be non-specific reactions of anti-nAChR  $\beta 4$  antibody because these bands were also seen in mock-transfected cells. To detect the co-expression of  $\alpha 3$  and  $\beta 4$  subunits on the cell surface, we performed immunofluorescence staining under non-permeable conditions using specific antibodies recognizing the extracellular epitope of  $\alpha 3$  or  $\beta 4$  subunit. Immunoreactivities of  $\alpha 3$  and  $\beta 4$  subunits were clearly detected in HEK293- $\alpha 3\beta 4$  cells, but not in mock-transfected cells (Fig. 3B).

### *3.3. Autoantibody-mediated internalization of cell-surface nAChR $\alpha 3$ subunits*

To assess the autoantibody-mediated internalization of cell-surface  $\alpha 3$  subunits, we incubated HEK293- $\alpha 3\beta 4$  cells with the patient's heat-inactivated serum at 4°C or 37°C. After 30-min incubation at 4°C, IgG was distributed uniformly over the cells (Fig. 4A). In contrast, after 30-min incubation at 37°C, IgG was detected as punctate dots (Fig. 4B). When the cells were incubated with rat anti-nAChR  $\alpha 3$  monoclonal antibodies (rat anti- $\alpha 3$ ) as a positive control, the formation of punctate dots of rat IgG occurred in a temperature-dependent manner, as seen for the patient's IgG (Fig. 4D and

E). Only a few punctate dots were seen under non-permeable staining conditions (data not shown), suggesting the internalization and intracellular localization of the patient's and rat IgG. Internalization of IgG was  $\alpha 3$  subunit-specific because no punctate dots were seen in mock-transfected cells incubated with both the patient's serum and rat anti- $\alpha 3$  (Fig. 4C and F). Punctate dots were not seen in the HEK293- $\alpha 3\beta 4$  cells incubated with normal serum (Fig. 5A).

Furthermore, we performed double-labeled immunofluorescence staining to examine the co-localization of internalized IgG and the  $\alpha 3$  subunit (Fig. 5). The  $\alpha 3$  subunit was stained using rabbit anti-nAChR  $\alpha 3$  antibody that recognizes different epitopes of rat anti- $\alpha 3$ . To test the time-dependent effect of IgG on  $\alpha 3$  subunit internalization, we compared the formation of overlapping staining at 5 min and 30 min after incubation. As observed in Fig. 4B and E, internalized patient's and rat IgG were detected as punctate dots. The  $\alpha 3$  subunits were also stained as a punctate pattern and overlapped with each IgG. The formation of overlapping punctate dots was observed in a time-dependent manner (Fig. 5A). Fig. 5B shows the quantitative results of overlapping punctate dot formation per cell at the indicated times after incubation.

HEK293- $\alpha 3\beta 4$  cells incubated with the patient's serum or rat anti- $\alpha 3$  for 5 min formed  $5.3 \pm 2.4$  or  $5.6 \pm 3.2$  punctate dots (n = 50), whereas those incubated for 30 min formed  $19.0 \pm 5.4$  or  $17.8 \pm 5.7$  punctate dots (n = 50), respectively (p<0.001). When the cells were incubated with normal serum, no punctate dot formation of IgG was observed, and  $\alpha 3$  subunits were diffusely stained over the cell. These results clearly suggested the autoantibody-mediated internalization of  $\alpha 3$  subunits.

#### **4. Discussion**

Autoantibody-mediated internalization of cell-surface antigen is now recognized as a key mechanism for some immune-mediated disorders, such as myasthenia gravis (MG) (Drachman et al., 1978), anti-N-methyl-D-aspartate receptor encephalitis (Hughes et al., 2010) and neuromyelitis optica (Hinson et al., 2012). In this study, we directly showed the involvement of autoantibodies in the internalization of nAChR  $\alpha 3$  subunit *in vitro*.

In the first part of this study, we demonstrated the affinity of the patient's IgG3 for  $\alpha 3$  subunit using immunofluorescence staining and immunoblot analysis. The

commonly used assay for the detection of anti-nAChR  $\alpha 3$  subunit autoantibody is radioimmunoprecipitation (RIP) using iodine 125 ( $^{125}\text{I}$ )-labeled epibatidine, a potent but non-selective agonist for neuronal nAChR, and solubilized neuronal nAChR from human neuroblastoma IMR-32 cells as antigenic sources (Vernino et al., 2000). IMR-32 cells are confirmed to express at least six neuronal nAChR subunits:  $\alpha 3$ ,  $\alpha 4$ ,  $\alpha 5$ ,  $\alpha 7$ ,  $\beta 2$  and  $\beta 4$  (Groot Kormelink and Luyten, 1997). Although autoantibodies detected in this RIP assay have been suggested to be highly specific for  $\alpha 3$  subunit, cross-reaction between different nAChR subunits can occur (Balestra et al., 2000; Vernino et al., 2008; Baker et al., 2009). In contrast, the immunofluorescence staining and immunoblot analysis established in this study can determine both the subunit specificity and the IgG subclass of the autoantibodies. Differences in these factors of autoantibody could affect the diversity of clinical symptoms between seropositive patients. Therefore, our assay methods may contribute to our understanding of the pathogenic roles of the autoantibody against neuronal nAChRs.

In contrast to anti-nAChR  $\alpha 3$  subunit autoantibody, pathogenic roles of anti-muscle nAChR autoantibodies in MG patients have been well characterized.

Accumulating evidence suggests that the following three effects are major contributing factors to MG pathogenesis (Keefe et al., 2009). When bound to muscle nAChR, autoantibodies induce (1) blocking of the cholinergic neurotransmission at neuromuscular junction (Drachman et al., 1982), (2) cross-linking and internalization of the muscle nAChR (Drachman et al., 1978) and (3) complement-dependent cell damage (Engel et al., 1979). On the other hand, some electrophysiological studies demonstrated that the anti-nAChR  $\alpha 3$  subunit autoantibody impaired the synaptic transmission (Lennon et al., 2003; Vernino et al., 2004), probably by mechanisms involving the autoantibody-mediated blocking and/or internalization of functional nAChR on the cell surface as reported in MG. In this study, we performed the assay for autoantibody-mediated internalization of nAChR using a seropositive patient's serum. For this assay, we established HEK293 cells stably co-expressing  $\alpha 3$  and  $\beta 4$  subunits (HEK293- $\alpha 3\beta 4$  cells). In accordance with previous reports that  $\alpha 3$  subunits could form functional receptors when expressed in combination with  $\beta 4$  subunits on the HEK293 cell surface (Krashia et al., 2010), we successfully co-expressed the  $\alpha 3$  and  $\beta 4$  subunits on the surface of HEK293 cells. When the HEK293- $\alpha 3\beta 4$  cells were

incubated with the patient's serum, antibody-mediated internalization of  $\alpha 3$  subunits was observed within 30 min, as predicted by a previous study (Wang et al., 2007). We also demonstrated the internalization of  $\alpha 3$  subunits using rat anti-nAChR  $\alpha 3$  monoclonal antibody as a positive control. This result suggests that antibodies against the extracellular domain of the  $\alpha 3$  subunit can induce internalization of the cell-surface  $\alpha 3$  subunit. Internalization of antibody was remarkably inhibited at low temperature, indicating that autoantibodies could be internalized via endocytosis because endocytic membrane trafficking is inhibited at low temperature (Arancibia-Carcamo et al., 2006).

On the other hand, it also remains to be seen whether complement-mediated neuronal cell damage is involved in the progression of neuronal symptoms. Some recent studies suggested that long-standing exposure to anti-nAChR  $\alpha 3$  subunit autoantibodies may cause the loss of neuronal cells and irreversible neuronal cell damage (Koike et al., 2010; Manganelli et al., 2011). In this study, we detected the IgG3 subclass autoantibody, which activates complement, in the patient's serum.

Although we have not examined the complement-dependent cell damage, differences in

IgG subclasses of autoantibodies could underlie the variety of clinical symptoms in seropositive patients.

In conclusion, we obtained evidence that autoantibodies against nAChR  $\alpha 3$  subunit induced the internalization of cell-surface nAChR. Our results support the hypothesis that the internalization of cell-surface nAChR is involved in the pathogenesis of the autoantibody against the nAChR  $\alpha 3$  subunit. However, this study was restricted in that serum was only obtained from one seropositive patient. Further accumulation of patients and pathophysiological evaluation should be carried out in future studies.

## **Acknowledgement**

This work was supported in part by a Health and Labour Sciences Research Grant on Intractable Diseases (Neuroimmunological Diseases) from the Ministry of Health, Labour and Welfare of Japan, and KAKENHI (24591253).

## References

- Albuquerque, E.X., Pereira, E.F., Alkondon, M., Rogers, S.W., 2009. Mammalian nicotinic acetylcholine receptors: from structure to function. *Physiol Rev.* 89, 73-120.
- Arancibia-Carcamo, I.L., Fairfax, B.P., Moss, S.J., Kittler, J.T., 2006. Studying the Localization, Surface Stability and Endocytosis of Neurotransmitter Receptors by Antibody Labeling and Biotinylation Approaches. In: Kittler, J.T., Moss, S.J. (Eds.), *The Dynamic Synapse: Molecular Methods in Ionotropic Receptor Biology*, *Frontiers in Neuroscience*, Boca Raton (FL).
- Baker, S.K., Morillo, C., Vernino, S., 2009. Autoimmune autonomic ganglionopathy with late-onset encephalopathy. *Auton Neurosci.* 146, 29-32.
- Balestra, B., Moretti, M., Longhi, R., Mantegazza, R., Clementi, F., Gotti, C., 2000. Antibodies against neuronal nicotinic receptor subtypes in neurological disorders. *J Neuroimmunol.* 102, 89-97.
- Drachman, D.B., Angus, C.W., Adams, R.N., Michelson, J.D., Hoffman, G.J., 1978. Myasthenic antibodies cross-link acetylcholine receptors to accelerate

degradation. *N Engl J Med.* 298, 1116-1122.

Drachman, D.B., Adams, R.N., Josifek, L.F., Self, S.G., 1982. Functional activities of autoantibodies to acetylcholine receptors and the clinical severity of myasthenia gravis. *N Engl J Med.* 307, 769-775.

Engel, A.G., Sakakibara, H., Sahashi, K., Lindstrom, J.M., Lambert, E.H., Lennon, V.A., 1979. Passively transferred experimental autoimmune myasthenia gravis. Sequential and quantitative study of the motor end-plate fine structure and ultrastructural localization of immune complexes (IgG and C3), and of the acetylcholine receptor. *Neurology.* 29, 179-188.

Flores, C.M., DeCamp, R.M., Kilo, S., Rogers, S.W., Hargreaves, K.M., 1996. Neuronal nicotinic receptor expression in sensory neurons of the rat trigeminal ganglion: demonstration of alpha3beta4, a novel subtype in the mammalian nervous system. *J Neurosci.* 16, 7892-7901.

Genzen, J.R., Van Cleve, W., McGehee, D.S., 2001. Dorsal root ganglion neurons express multiple nicotinic acetylcholine receptor subtypes. *J Neurophysiol.* 86, 1773-1782.

- Gibbons, C.H., Centi, J., Vernino, S., Freeman, R., 2012. Autoimmune autonomic ganglionopathy with reversible cognitive impairment. *Arch Neurol.* 69, 461-466.
- Groot Kormelink, P.J., Luyten, W.H., 1997. Cloning and sequence of full-length cDNAs encoding the human neuronal nicotinic acetylcholine receptor (nAChR) subunits beta3 and beta4 and expression of seven nAChR subunits in the human neuroblastoma cell line SH-SY5Y and/or IMR-32. *FEBS Lett.* 400, 309-314.
- Hinson, S.R., Romero, M.F., Popescu, B.F., Lucchinetti, C.F., Fryer, J.P., Wolburg, H., Fallier-Becker, P., Noell, S., Lennon, V.A., 2012. Molecular outcomes of neuromyelitis optica (NMO)-IgG binding to aquaporin-4 in astrocytes. *Proc Natl Acad Sci U S A.* 109, 1245-1250.
- Hughes, E.G., Peng, X., Gleichman, A.J., Lai, M., Zhou, L., Tsou, R., Parsons, T.D., Lynch, D.R., Dalmau, J., Balice-Gordon, R.J., 2010. Cellular and synaptic mechanisms of anti-NMDA receptor encephalitis. *J Neurosci.* 30, 5866-5875.
- Keefe, D., Hess, D., Bosco, J., Tzartos, S., Powell, J., Lamsa, J., Josiah, S., 2009. A rapid, fluorescence-based assay for detecting antigenic modulation of the acetylcholine receptor on human cell lines. *Cytometry B Clin Cytom.* 76,

206-212.

Khan, I., Osaka, H., Stanislaus, S., Calvo, R.M., Deerinck, T., Yaksh, T.L., Taylor, P.,

2003. Nicotinic acetylcholine receptor distribution in relation to spinal

neurotransmission pathways. *J Comp Neurol.* 467, 44-59.

Klein, C.M., Vernino, S., Lennon, V.A., Sandroni, P., Fealey, R.D., Benrud-Larson, L.,

Sletten, D., Low, P.A., 2003. The spectrum of autoimmune autonomic

neuropathies. *Ann Neurol.* 53, 752-758.

Koike, H., Koyano, S., Morozumi, S., Kawagashira, Y., Iijima, M., Katsuno, M.,

Hattori, N., Vernino, S., Sobue, G., 2010. Slowly progressive autonomic

neuropathy with antiganglionic acetylcholine receptor antibody. *J Neurol*

*Neurosurg Psychiatry.* 81, 586-587.

Krashia, P., Moroni, M., Broadbent, S., Hofmann, G., Kracun, S., Beato, M.,

Groot-Kormelink, P.J., Sivilotti, L.G., 2010. Human alpha3beta4 neuronal

nicotinic receptors show different stoichiometry if they are expressed in

*Xenopus* oocytes or mammalian HEK293 cells. *PLoS One.* 5, e13611.

Lennon, V.A., Ermilov, L.G., Szurszewski, J.H., Vernino, S., 2003. Immunization with

neuronal nicotinic acetylcholine receptor induces neurological autoimmune disease. *J Clin Invest.* 111, 907-913.

Lykhmus, O., Koval, L., Skok, M., Zouridakis, M., Zisimopoulou, P., Tzartos, S., Tsetlin, V., Granon, S., Changeux, J.P., Komisarenko, S., Cloez-Tayarani, I., 2011. Antibodies against extracellular domains of alpha4 and alpha7 subunits alter the levels of nicotinic receptors in the mouse brain and affect memory: possible relevance to Alzheimer's pathology. *J Alzheimers Dis.* 24, 693-704.

Manganelli, F., Dubbioso, R., Nolano, M., Iodice, R., Pisciotta, C., Provitera, V., Ruggiero, L., Serlenga, L., Barbieri, F., Santoro, L., 2011. Autoimmune autonomic ganglionopathy: a possible postganglionic neuropathy. *Arch Neurol.* 68, 504-507.

McKeon, A., Lennon, V.A., Lachance, D.H., Fealey, R.D., Pittock, S.J., 2009. Ganglionic acetylcholine receptor autoantibody: oncological, neurological, and serological accompaniments. *Arch Neurol.* 66, 735-741.

Mizushima, S., Nagata, S., 1990. pEF-BOS, a powerful mammalian expression vector. *Nucleic Acids Res.* 18, 5322.

- Skok, V.I., 2002. Nicotinic acetylcholine receptors in autonomic ganglia. *Auton Neurosci.* 97, 1-11.
- Vernino, S., Adamski, J., Kryzer, T.J., Fealey, R.D., Lennon, V.A., 1998. Neuronal nicotinic ACh receptor antibody in subacute autonomic neuropathy and cancer-related syndromes. *Neurology.* 50, 1806-1813.
- Vernino, S., Low, P.A., Fealey, R.D., Stewart, J.D., Farrugia, G., Lennon, V.A., 2000. Autoantibodies to ganglionic acetylcholine receptors in autoimmune autonomic neuropathies. *N Engl J Med.* 343, 847-855.
- Vernino, S., Ermilov, L.G., Sha, L., Szurszewski, J.H., Low, P.A., Lennon, V.A., 2004. Passive transfer of autoimmune autonomic neuropathy to mice. *J Neurosci.* 24, 7037-7042.
- Vernino, S., Lindstrom, J., Hopkins, S., Wang, Z., Low, P.A., 2008. Characterization of ganglionic acetylcholine receptor autoantibodies. *J Neuroimmunol.* 197, 63-69.
- Wang, Z., Low, P.A., Jordan, J., Freeman, R., Gibbons, C.H., Schroeder, C., Sandroni, P., Vernino, S., 2007. Autoimmune autonomic ganglionopathy: IgG effects on ganglionic acetylcholine receptor current. *Neurology.* 68, 1917-1921.

Wang, Z., Low, P.A., Vernino, S., 2010. Antibody-mediated impairment and homeostatic plasticity of autonomic ganglionic synaptic transmission. *Exp Neurol.* 222, 114-119.

Winston, N., Vernino, S., 2010. Recent advances in autoimmune autonomic ganglionopathy. *Curr Opin Neurol.* 23, 514-518.

## Figure Legends

**Fig. 1.** Detection of autoantibodies against neuronal nAChR subunits by double-labeled immunofluorescence staining. (A) COS-7 cells transiently expressing  $\alpha 3$  subunit were stained with the patient's serum (top) and normal serum (bottom). IgG, human IgG detected with DyLight 488-conjugated anti-human IgG antibody (green);  $\alpha 3$ , commercially available anti-nAChR  $\alpha 3$  antibody detected with Alexa Fluor 594-conjugated anti-rabbit IgG antibody (red); Merge, merged images (yellow). Nuclei were stained with DAPI (blue). Note that staining of IgG was detectable from the patient's serum, but not from normal control. (B) Relationship between serum dilution and relative fluorescent intensity. Abscissa, serum dilution; ordinate, relative intensity. The fluorescent intensity for human IgG (green) was normalized to that for nAChR  $\alpha 3$  (red). (C) COS-7 cells transiently expressing nAChR  $\alpha 4$ ,  $\alpha 5$ ,  $\alpha 7$ ,  $\beta 2$  and  $\beta 4$  subunits were stained with the patient's serum and commercially available antibodies specific for the indicated subunits as described above for  $\alpha 3$ . Merged images are shown. Note that no staining of human IgG (green) is detectable. Scale bars, 50  $\mu\text{m}$ .

**Fig. 2.** Detection of anti-nAChR  $\alpha 3$  autoantibodies by immunoblot analysis. (A)

Detection with rabbit anti-nAChR  $\alpha 3$  subunit (Rabbit anti- $\alpha 3$ ). Homogenates (1  $\mu\text{g}$  of protein) prepared from COS-7 cells transiently transfected with pEF-CHRNA3 ( $\alpha 3$ ) and empty vector (Mock) subjected to immunoblot analysis as described in the Materials and methods. Note that two bands of 55 and 50 kD are specifically detected for pEF-CHRNA3-transfected cells. (B) Detection with the patient's serum. Note that two bands of 55 and 50 kD as in (A) are detectable with anti-human IgG3 antibody, but not with anti-human IgG1, 2 and 4 antibodies. The positions of molecular weight markers (kD) are indicated on the left.

**Fig. 3.** Establishment of human embryonic kidney (HEK) 293 cells stably

co-expressing nAChR  $\alpha 3$  and  $\beta 4$  subunits. (A) Immunoblot analysis of homogenates (10  $\mu\text{g}$  of protein) from HEK293 cells stably co-transfected with pcDNA-CHRNA3 and pcDNA-CHRNB4 ( $\alpha 3\beta 4$ ) and those with empty vector (Mock). The blots were probed with rabbit anti-nAChR  $\alpha 3$  antibody (Anti- $\alpha 3$ ) or rabbit anti-nAChR  $\beta 4$

antibody (Anti- $\beta$ 4). The positions of molecular weight markers (kD) are indicated.

(B) Immunofluorescence staining of HEK293- $\alpha$ 3 $\beta$ 4 cells ( $\alpha$ 3 $\beta$ 4) and mock-transfected cells (Mock). Cells were stained with rat anti-nAChR  $\alpha$ 3 (Anti- $\alpha$ 3) and rabbit anti-nAChR  $\beta$ 4 (Anti- $\beta$ 4) under non-permeable staining conditions, and detected with Alexa Fluor 488-conjugated anti-rat IgG antibody (green) and Alexa Fluor 594-conjugated anti-rabbit IgG antibody (red), respectively. Nuclei were stained with DAPI (blue). Scale bar, 100  $\mu$ m.

**Fig. 4.** Detection of internalized human and rat IgG in HEK293 cells stably co-expressing nAChR  $\alpha$ 3 and  $\beta$ 4 subunits by immunofluorescence staining. HEK293 cells stably expressing both  $\alpha$ 3 and  $\beta$ 4 subunits (HEK293- $\alpha$ 3 $\beta$ 4) and mock-transfected cells (Mock) were incubated with the patient's serum (A–C) or rat anti-nAChR  $\alpha$ 3 monoclonal antibody (Rat anti- $\alpha$ 3; D–F) for 30 min at 4°C or 37°C. Cells were then fixed, permeabilized and stained with DyLight 488-conjugated anti-human IgG antibody (A–C) or Alexa Fluor 488-conjugated anti-rat IgG antibody (D–F). Note that

punctate staining of both patient's and rat IgG is detectable in HEK293- $\alpha3\beta4$  cells at 37°C, but not at 4°C. Scale bar, 20  $\mu\text{m}$ .

**Fig. 5.** Co-localization of internalized human and rat IgG with nAChR  $\alpha3$  subunit in HEK293 cells stably co-expressing  $\alpha3$  and  $\beta4$  subunits (HEK293- $\alpha3\beta4$ ). (A) Cells were incubated with the patient's serum, normal control serum or rat anti-nAChR  $\alpha3$  monoclonal antibody (Rat anti- $\alpha3$ ) for 5 min and 30 min at 37°C. Then, the cells were fixed, permeabilized and stained with rabbit anti-nAChR  $\alpha3$  antibody, followed by detection with DyLight 488-conjugated anti-human IgG or Alexa Fluor 488-conjugated anti-rat IgG (green), and Alexa Fluor 488-conjugated anti-rabbit IgG (red). Nuclei were stained with DAPI (blue). Scale bar, 20  $\mu\text{m}$ . (B) The number of overlapping punctate dots formed by patient's serum and rat anti- $\alpha3$  was counted at the indicated time points. Data are expressed as mean  $\pm$  S.D.; \*,  $p < 0.001$ , two-tailed  $t$ -test. Note that overlapping punctate dots were observed in the cells incubated with the patient's serum and rat anti- $\alpha3$ , and increased in a time-dependent manner. No overlapping staining was observed in the cells incubated with normal serum.

Table 1

Primers used for amplification of cDNAs encoding human nAChR subunits

Subunit	Sequence (5'–3')	
$\alpha 3$	F1: ggtctggggtctcgctgga	F2: gagaggccgtctctcgacc
	R1: gaagcagcctcctcctgccc	R2: ggcaggcacacagcttagtgc
$\alpha 4$	F1: cccacaggagaagacgaac	F2: catctagagcccgcgaggtg
	R1: ccaaggccgtttacagcag	R2: gagtccaggagaagccagc
$\alpha 5$	F1: cagcactcacactcagtctc	F2: aagagttcgcgttccccgcg
	R1: atagtgccatcagatatatgtgtg	R2: acttcagtccttgggaggc
$\alpha 7$	F1: gcgacagccgagacgtggag	F2: gctgcagctccgggactcaa
	R1: gtggcgtgtaatgctgtcctgg	R2: ggccttgccatctgtgagt
$\beta 2$	F1: ggcttcagcaccacggacag	F2: ggtgtaggcgaggcagcgag
	R1: gccctcttctggtagctc	R2: tactgtgcagcagagggtggc
$\beta 4$	F1: aggaccggcgtcactcgac	F2: tgtgacccacagcgagct
	R1: gggcctcatcagccacaacc	R2: ctctaccccaaccagg

F1 and R1 refer to forward and reverse primers for the 1st PCR; F2 and R2 to those for the 2nd PCR.

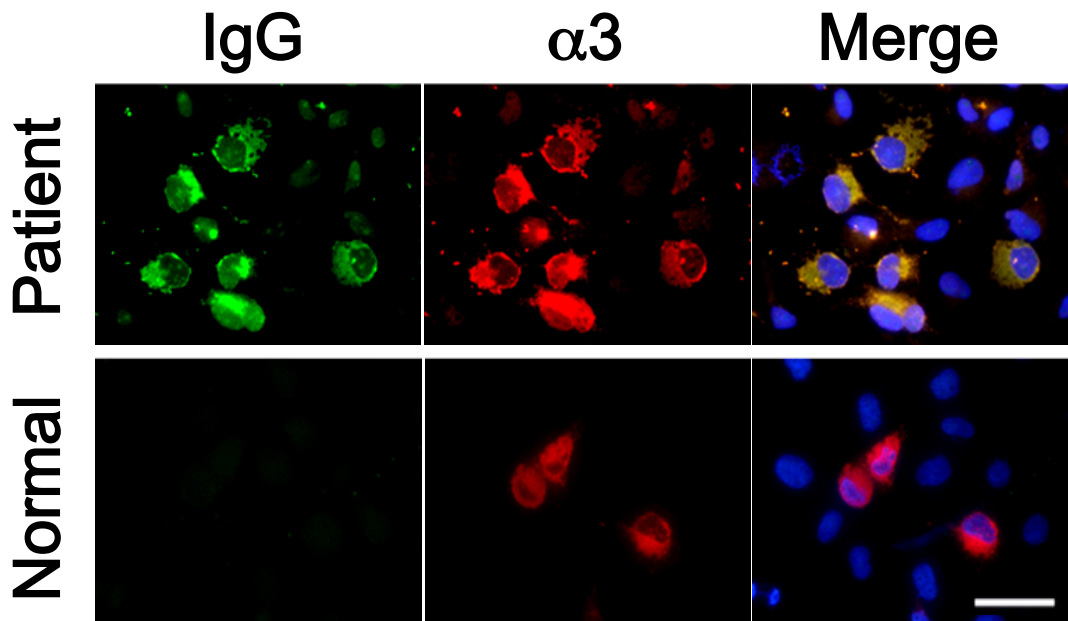
Table 2. List of antibodies used in this study

Antibody	Species / Clonality	Source (Catalogue No.)	Dilution	Usage
<b>Primary antibodies</b>				
Anti-nAChR $\alpha$ 3 subunit	Rabbit / Polyclonal	Santa Cruz (sc-5590)	1:1,000	IF, IB
Anti-nAChR $\alpha$ 4 subunit	Goat / Polyclonal	Santa Cruz (sc-1772)	1:1,000	IF
Anti-nAChR $\alpha$ 5 subunit	Rabbit / Polyclonal	Abcam (ab26099)	1:1,000	IF
Anti-nAChR $\alpha$ 7 subunit	Goat / Polyclonal	Santa Cruz (sc-1447)	1:1,000	IF
Anti-nAChR $\beta$ 2 subunit	Rabbit / Polyclonal	Santa Cruz (sc-11372)	1:1,000	IF
Anti-nAChR $\beta$ 4 subunit	Rabbit / Polyclonal	Millipore (AB15327)	1:2,000	IF, IB
Anti-nAChR $\alpha$ 1, $\alpha$ 3, $\alpha$ 5 subunit	Rat / Monoclonal	Abcam (ab24719)	1:1,000	IF
<b>Secondary antibodies</b>				
Alexa Fluor 594-conjugated anti-rabbit IgG	Donkey	Invitrogen (A21207)	1:2,000	IF
Alexa Fluor 594-conjugated anti-goat IgG	Donkey	Invitrogen (A11058)	1:2,000	IF
Alexa Fluor 594-conjugated anti-rat IgG	Donkey	Invitrogen (A21209)	1:2,000–5,000	IF
Alexa Fluor 488-conjugated anti-rabbit IgG	Donkey	Invitrogen (A21206)	1:2,000	IF
DyLight 488-conjugated anti-human IgG	Donkey	Jackson ImmunoRes.Lab. (709-486-149)	1:2,000	IF
Alkaline-phosphatase-conjugated anti-rabbit IgG	Goat	BIO-RAD (170-6518)	1:2,000	IB
Alkaline-phosphatase-conjugated anti-human IgG1	Mouse	Merck KGaA (401459)	1:5,000	IB
anti-human IgG2	Mouse	Merck KGaA (401462)	1:5,000	IB
anti-human IgG3	Mouse	Merck KGaA (401465)	1:5,000	IB
anti-human IgG4	Mouse	Merck KGaA (401468)	1:5,000	IB

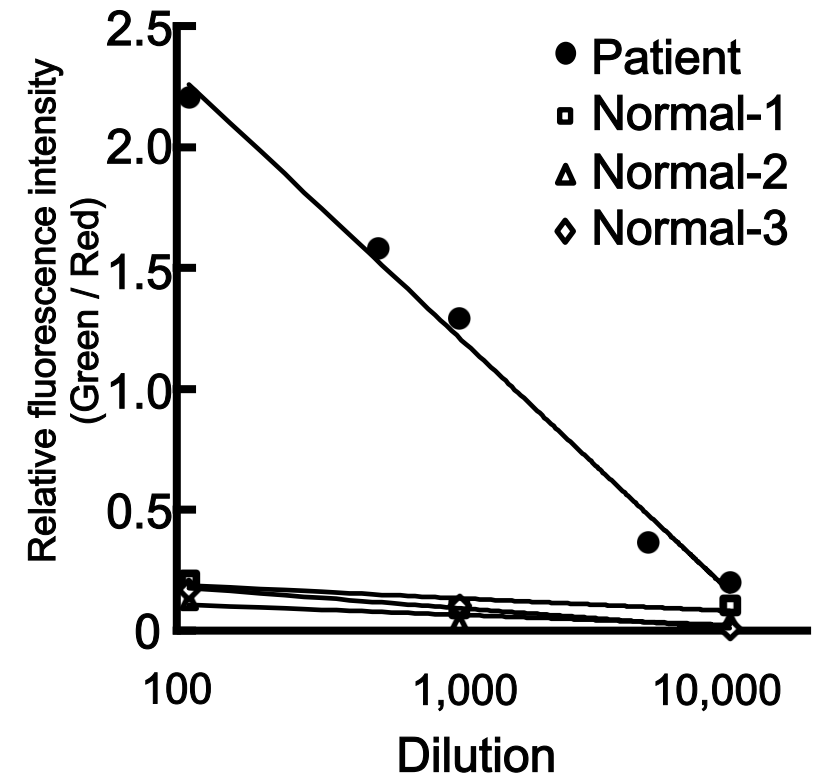
IF, immunofluorescence staining; IB, immunoblot analysis

Fig. 1.

**A**



**B**



**C**

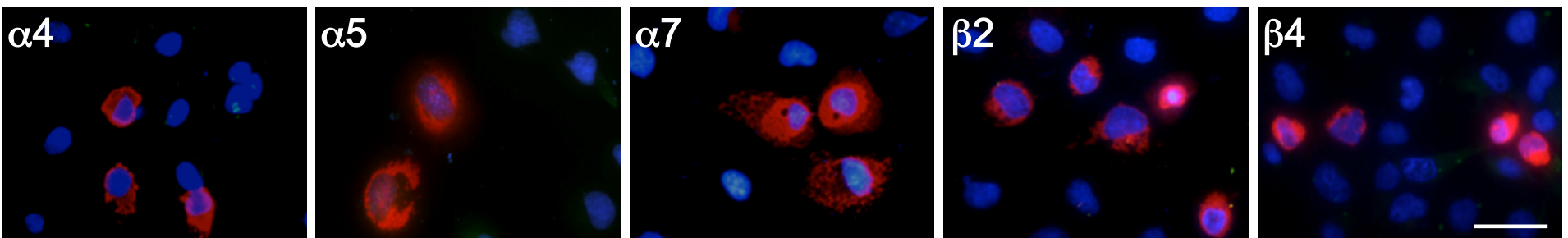
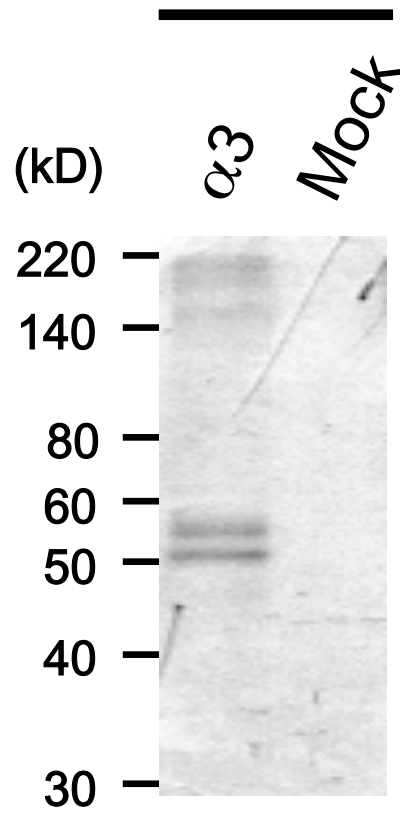


Fig. 2.

**A**

Rabbit anti- $\alpha$ 3



**B**

Patient's serum

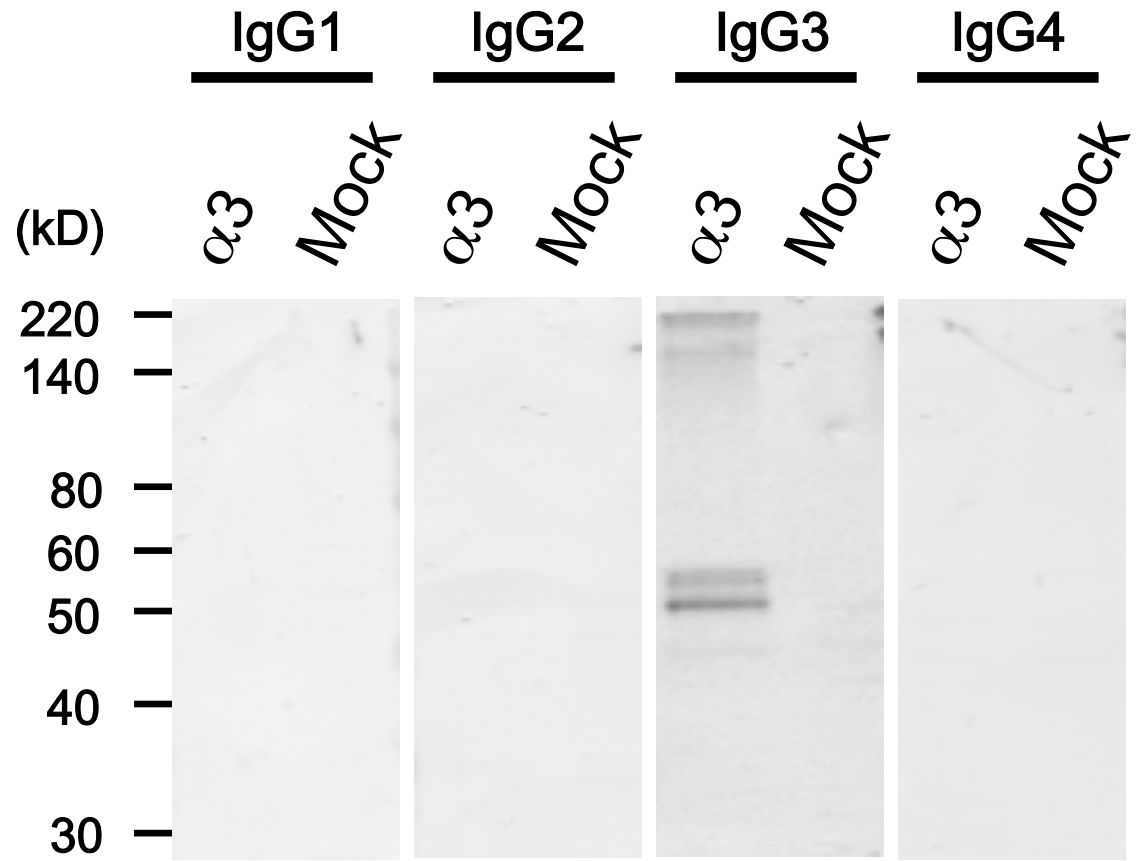


Fig. 3.

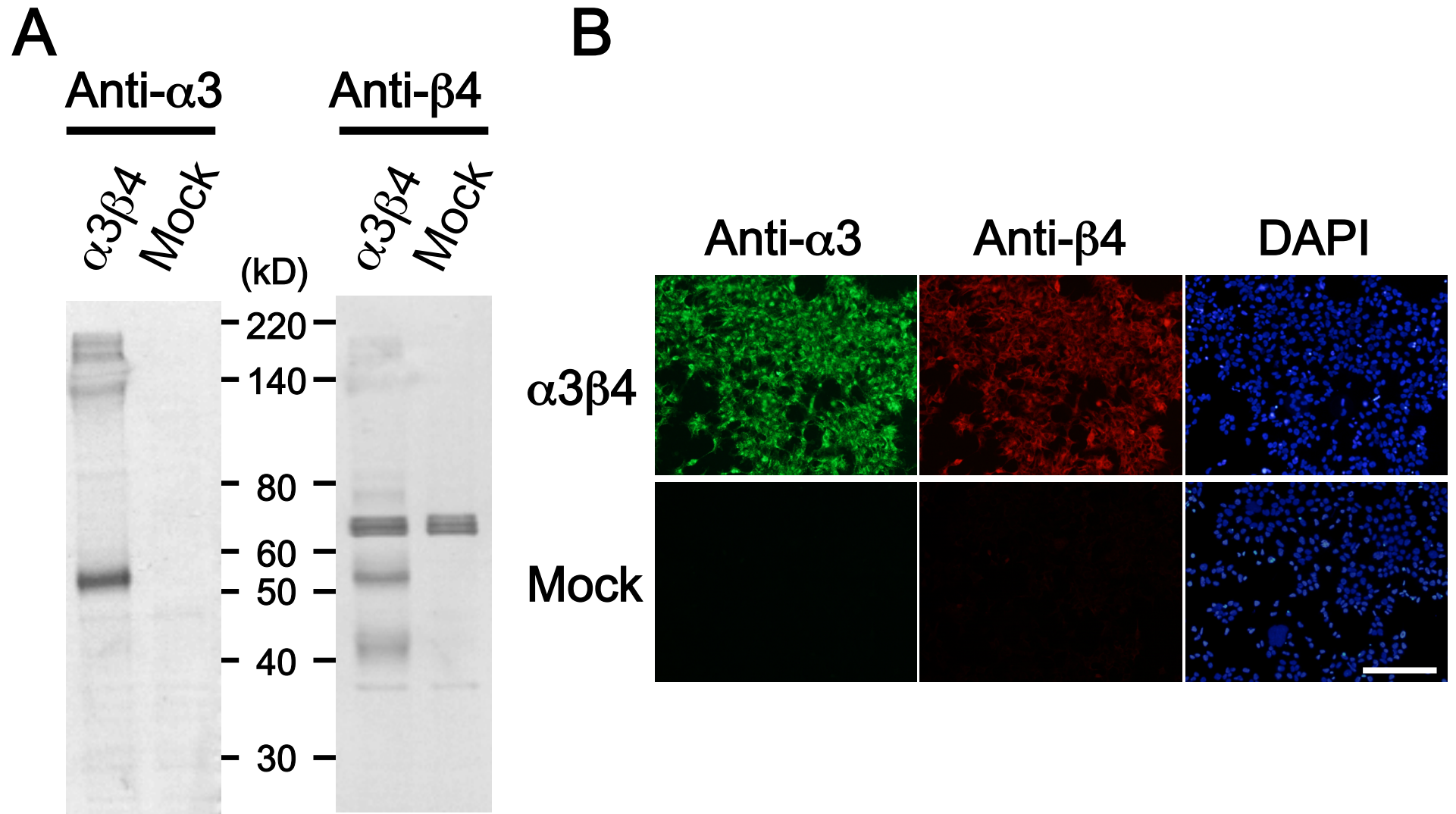


Fig. 4.

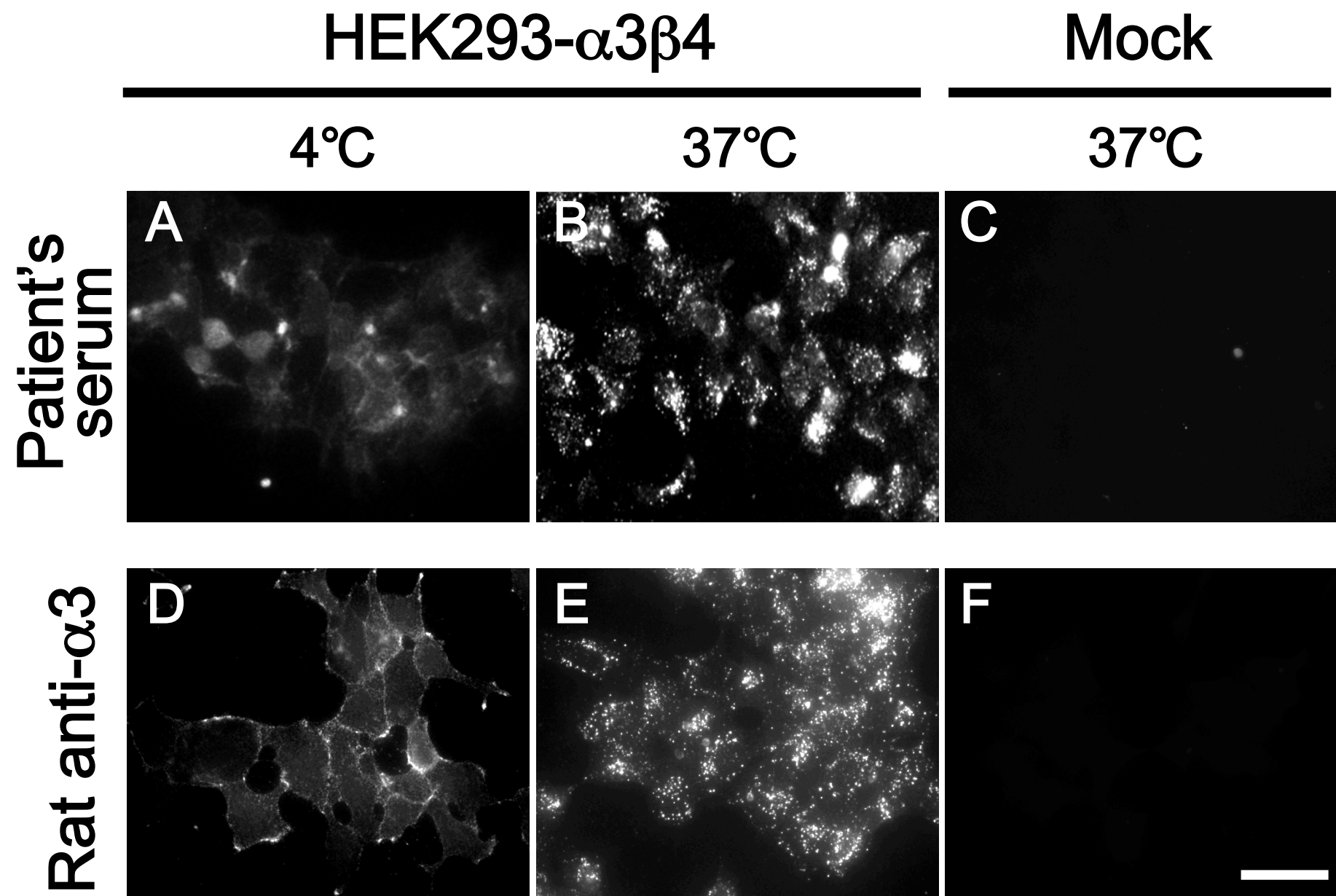
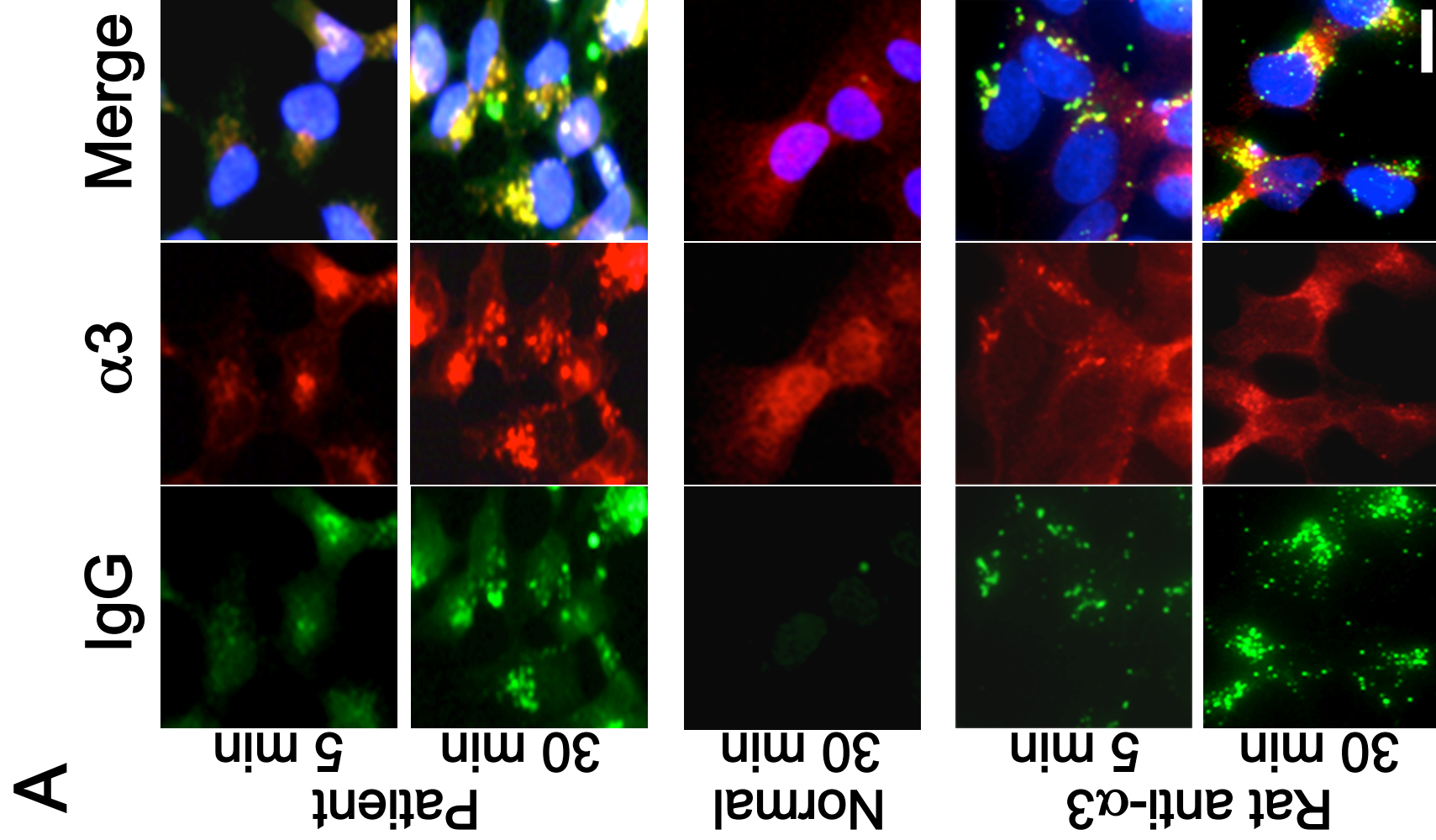


Fig. 5.



**B**

